Deformation increase of high-spin core-excited isomers in the astatine nuclei

G. Scheveneels, F. Hardeman, G. Neyens, and R. Coussement
Katholieke Universiteit Leuven, Celestijnenlaan 200 D, B-3001 Leuven, Belgium
(Received 1 February 1989; revised manuscript received 1 September 1989)

Quadrupole moments of six high-spin isomers in the At isotopes have been measured with the level-mixing-spectroscopy method: ^{208}At(16^-), ^{209}At($\frac{29}{2}^+$), ^{210}At($19^+,15^-$), ^{211}At($\frac{39}{2}^-,\frac{29}{2}^+$). The results show that level mixing spectroscopy is a promising technique to determine quadrupole moments of isomers that are difficult to measure by other in-beam hyperfine interaction methods. A large increase of the quadrupole moment is observed if neutrons are excited across or removed from the $N=126$ shell closure. This behavior is explained in terms of an enhanced core softness for fewer core neutrons; the aligned valence particles, moving in equatorial orbits, then easily polarize the core towards oblate deformation.

I. INTRODUCTION

High-spin yrast traps, where the high spin is built up by the alignment of single-particle angular momentum, are of current theoretical interest.[1,2] Because of their isomeric character, a number of nuclear parameters can be measured for these states. Whereas energy, magnetic dipole moments, and spins provide valuable information on the particle configuration of these states, electric quadrupole moments are very sensitive to the collective deformation of the core.

Until now, in-beam quadrupole moment measurements on high-spin isomers are almost exclusively performed by time-differential perturbed angular distribution (TDPAD).[3,4] The TDPAD method becomes increasingly difficult for higher spins[5] and lifetimes larger than several microseconds. For this reason our group developed the level-mixing-spectroscopy (LEMS) technique, which is extensively discussed in Ref. 5. It has the advantage of not becoming more difficult for higher spins, and it is applicable to a broad lifetime range for which the upper limit is only limited by thermal spin-lattice relaxation. The results reported in this paper clearly demonstrate the high-spin feature of LEMS.

The high-spin yrast traps in the mass region of ^{208}Pb have been studied extensively during the past few years. For their theoretical description, two models are frequently applied. The spherical shell model with empirical residual interactions is very successful in the description of the valence particle properties of these states; see, for example, Refs. 6 and 7. The other model is a Nilsson-type model of independent particles moving in a deformed potential, similar to the model that has been applied to explain the strongly deformed nuclei in the Gd region.[8] Because of the small deformations involved in the Pb region, a linear approximation has been developed by Matsuyanagi, Døssing, and Neergård,[9] the deformed-independent-particle model (DIPM). Both pictures, the one of independent particles moving in a deformed potential and the other of a few interacting valence particles moving in a spherical potential, predict the same general behavior for the energy levels,[9] but differ substantially in their prediction of the quadrupole moments. The already measured moments favor the DIPM model; although the theoretically predicted core deformation is too large, the increasing core softness as neutrons are removed from the $N=126$ shell closure is well-established experimentally.[3,4]

At very high spin, core-excited neutrons are needed to build up the spin. If this happens, the polarizing effect should greatly increase, since, in addition to the presence of an extra polarizing particle, the magic core has been broken. The only core-excited state hitherto measured is the $\frac{63}{2}^-$ state in ^{211}Rn.[12] However, the small core deformation derived from those data [$\beta=-0.03(1)$] seems to contradict the predictions.

In this paper we report on the quadrupole moments of core-excited isomers in the At isotopes. In addition, we have also measured the Q moment of isomers previously known and these serve as a check of our new method.

II. EXPERIMENTAL PROCEDURE

All isomers (Fig. 1) were populated and aligned by the ^{209}Bi(α,xn) reaction (Table I), with alpha beams of different energy from the cyclotron Cyclone of the UCL University (Belgium). Beam pulsing was applied to prevent the acquisition of fast gamma rays not originating from the decay of an isomer; data acquisition was done only during the beam-off period, which was chosen comparable with the lifetime of the investigated isomer. This pulsing had no influence on the LEMS measurement.[5] Since Bi has a rhombohedral structure, the target is also used as the recoil and host material to provide an axially symmetric quadrupole interaction. In all experiments a polycrystalline Bi target of about 1 mm thick was used. To anneal possible radiation damage, the target was heated to a temperature near the melting point of Bi; at this temperature no radiation-damage effects were observed in TDPAD experiments.[13]

The magnetic field parallel with the beam axis is generated by a split-coil superconducting magnet with a

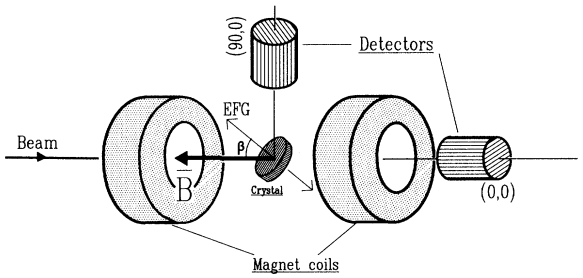

FIG. 1. Experimental setup for a LEMS experiment.

maximum field of 5 T (Fig. 2). Gamma rays were detected by two high-purity n-type Ge detectors, one behind the magnet at 0° and the other one perpendicular to the magnetic-field axis. To cancel beam intensity fluctuations, the ratio of the counts of the two detectors $[N(0°)/N(90°)]$ was taken. This ratio is measured as a function of the magnetic-field strength and contains three free parameters: the ratio of the detection efficiencies, the initial anisotropy, and the ratio of the quadrupole to magnetic interaction strength. For a reliable uncorrelated determination of these parameters, the complete LEMS curve has to be measured: The zero-field point is most sensitive to the efficiency ratio; at high field the unperturbed anisotropy is measured, and the middle part of the curve is sensitive to the ratio of the quadrupole to magnetic interaction strength.

III. RESULTS

The experimental results are listed in Table II; for completeness and comparison the TDPAD values taken from Ref. 13 are also included. Some experimental LEMS curves, together with the numerical fit to the data, are shown in Fig. 3. The parameter derived from the LEMS curve is the ratio μ/ν_Q. The error on the interaction ratio is determined by a standard minimum χ^2 fit to the experimental data. The magnetic moments needed to extract the quadrupole interaction frequencies are included in Table II. The g factor of the 16^- isomer in ^{208}At has to our knowledge not yet been measured, and we have adopted a magnetic moment of

$$\mu(16^-)=0.9897\ \mu(^{209}\text{At}\ \tfrac{29}{2}^+)+0.6588\ \mu(^{207}\text{Pb}\tfrac{5}{2}^-)$$
$$=15.7\ \text{nm}\ ,$$

in order to extract the ν_Q value of the 16^- isomer in ^{208}At. As the uncertainty in the magnetic moments is much less than the error in the interaction ratio determined by LEMS, it is the LEMS measurement that determines the error in the ν_Q values.

Following Ref. 13, the electric-field gradient (EFG) of At in Bi is calibrated by using the $B(E2)$ value of the $\frac{21}{2}^- \rightarrow \frac{17}{2}^-$ transition in ^{211}At[18] and the assumed identical ratio of the quadrupole moments of the $\pi h_{9/2}^3$ and $\pi h_{9/2}^2 i_{13/2}$ isomers in ^{211,210,209}At. This derivation of the quadrupole moments is reliable, but not unquestionable; the relative values are, however, uniquely determined by experiment and reflect the essential behavior.

The quadrupole interaction frequencies measured by both TDPAD and LEMS agree fairly well, demonstrating the reliability of our new technique. The larger error obtained in the LEMS technique is partly due to the short counting time available for our experiments, but also due to the nonresonant and nonperiodic behavior of the LEMS signal. It should be pointed out, however, that the uncertainties for the high-spin isomers are no larger than for the low-spin states, whereas TDPAD measurements for high-spin states become exceedingly difficult.

IV. DISCUSSION

The high-spin isomers in the astatine isotopes can be divided into three groups with each approximately the same valence particle configuration. For each configuration the quadrupole moment significantly increases toward the more neutron-deficient isotopes (Figs. 4 and 5). This is evidence of an increasing core polarization when more neutrons are removed from the $N=126$ shell closure. However, the most striking behavior is the strong increase for the quadrupole moments of the core-excited states, the $\frac{39}{2}^-$ isomer in ^{211}At and the 19^+ isomer in ^{210}At. The core-excited states differ from the lower-lying isomers, the $\frac{29}{2}^+$ and 15^- isomers, by one

TABLE I. Experimental data.

Isomer	Reaction energy	Host Temp.	γ-energy (keV)	Multipolarity
^{211}At $\frac{29}{2}^+$ 70 ns	Bi(α,2n) 35 MeV	Bi poly 480 K	511	$M1$
^{211}At $\frac{39}{2}^-$ 4.2 μs	Bi(α,2n) 35 MeV	Bi poly 480 K	435	$E3$
^{210}At 15^- 580 ns	Bi(α,3n) 47 MeV	Bi poly 480 K	644	$E3$
^{210}At 19^+ 4.0 μs	Bi(α,3n) 47 MeV	Bi poly 480 K	371	$E3$
^{209}At $\frac{29}{2}^+$ 870 ns	Bi(α,4n) 55 MeV	Bi poly 480 K	424	$E2$
			578	$E3$
^{208}At 16^- 1.5 μs	Bi(α,5n) 73 MeV	Bi poly 480 K	472	$E3$
			751	$E3$

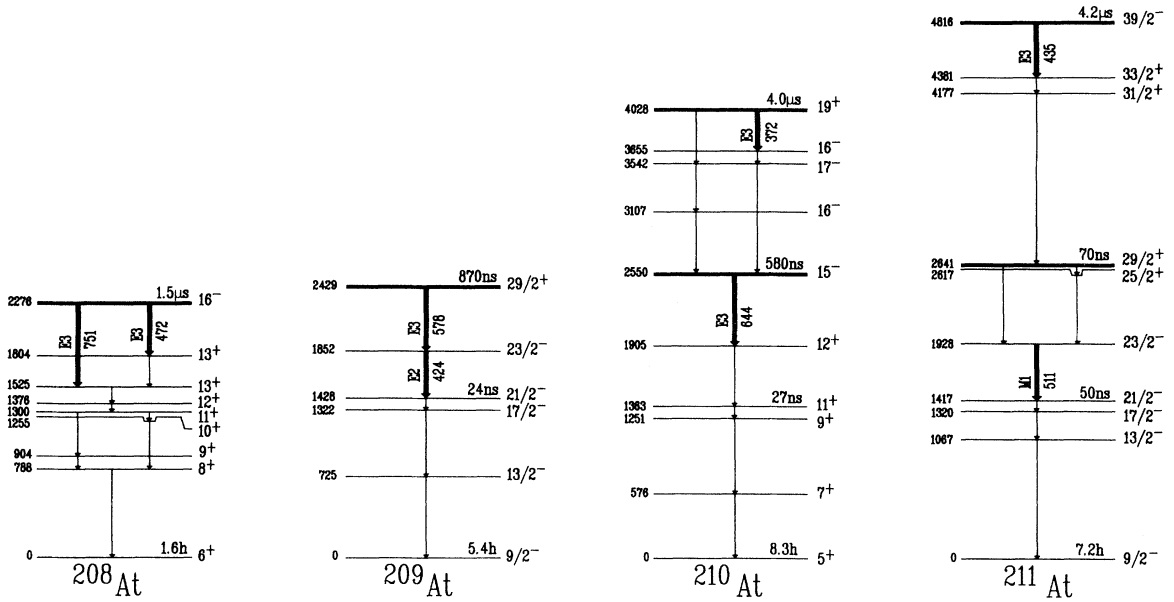

FIG. 2. Isomers in the At isotopes and their principal mode of decay.

$\nu p_{1/2}$ neutron that is excited to the $\nu g_{9/2}$ orbital above the $N=126$ gap. This neutron rearrangement does not directly affect the electric quadrupole moment, but results in a strongly enhanced core polarization. The increased core polarization has two reasons, which are respectively, the extra neutron hole in the $N=126$ shell by which the core softens and the extra valence neutron that contributes to the polarization of the core. These observations agree with the systematics predicted by the DIPM.

The preceding discussion is based on the relative behavior of the quadrupole moments and is independent of the calibration. We shall now proceed to a more quantitative examination. In Table III the experimental quadrupole moments are compared to several theoretical predictions. The shell-model configuration of the isomeric states is characterized by a stretched coupling of angular momenta. The quadrupole moment of the valence nucleons can then be unambiguously decomposed into single-particle moments. Different values for the quadrupole moments of the valence particles are used to obtain the results in Table III. The most basic approach is to use the spherical shell-model orbitals and bare charges for neutron and proton ($e_\pi=1$, $e_\nu=0$). The mean-square radii $\langle r^2 \rangle$ of the orbitals involved are taken from Ref. 19.

The quadrupole moments Q_p calculated with these pure valence particle quadrupole moments (Table IV) are certainly much too small (Table III); the deviation rapid-

TABLE II. Results of the LEMS and TDPAD measurements in the astatine isotopes.

Isomer	μ (μ_N)[a]	ν_Q (MHz)[b]	ν_Q (MHz)[c]	Q (fm^2)[d]
^{211}At $\frac{29}{2}^+$ 70 ns	15.31(13)	150(20)	163(7)	101(19)
^{211}At $\frac{39}{2}^-$ 4.2 μs	13.5(1)	305(25)		191(25)
^{210}At 11^+ 27 ns	9.79(33)		104(6)	65(8)
^{210}At 15^- 580 ns	15.57(15)	220(15)	196(2)	122(12)
^{210}At 19^+ 4 μs	13.26(13)	350(20)		220(5)
^{209}At $\frac{21}{2}^-$	9.98(21)		126(5)	78(8)
^{209}At $\frac{29}{2}^+$ 870 ns	15.38(14)	240(20)	242(2)	150(15)
^{208}At 16^- 1.5 μs	15.7	270(25)		169(25)

[a]The magnetic moments needed to extract ν_Q from the LEMS measurement are taken from Refs. 15 and 16.

[b]Results of the LEMS measurements.

[c]Results of the TDPAD measurements (Ref. 13).

[d]For those isomers for which a TDPAD measurement was already performed, the Q moment has been derived from their value. Calibration standard $Q(^{211}\text{At}, \frac{29}{2}^+)=101(19)$; see Ref. 13.

ly increases with the number of neutron holes present in the $N=126$ shell. For the two core-excited isomers, the $\frac{39}{2}^-$ isomer in ^{211}At and the 19^+ isomer in ^{210}At, the experimental Q moment is a factor of 3 larger than the pure spherical shell-model predictions. This is a strong indication for the polarizing effect of the valence particles in the core: Particles (holes) will polarize the core toward maximum (minimum) overlap with nuclear matter. The polarization effect results from a balance between the interaction energy gained by the valence particles and the increasing core deformation energy.

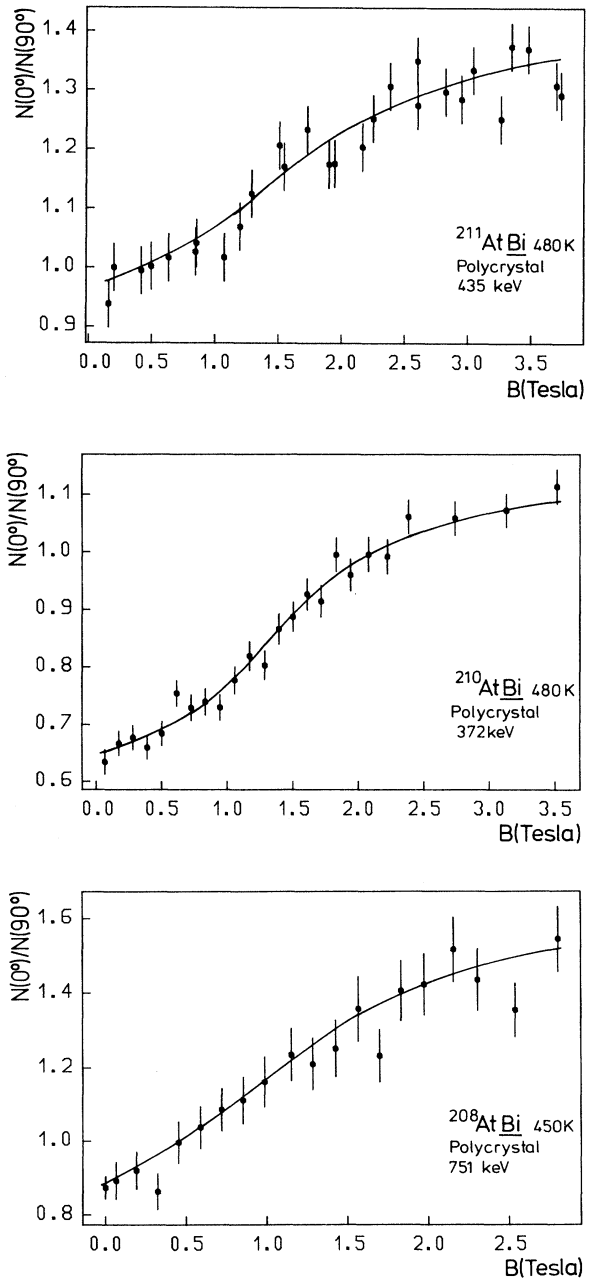

FIG. 3. Some experimental LEMS curves.

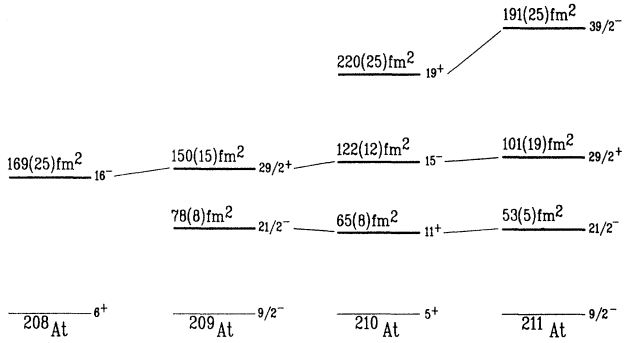

FIG. 4. Variation of the Q moments of the astatine isomers.

Sagawa and Arima calculated the admixture of giant resonances of the ^{208}Pb core with the valence particle orbitals; concerning the quadrupole moments, this effect is incorporated in an effective charge for the orbitals.[19] The Q_{eff} moments (Table III) are calculated with these effective charges for the valence particles and a much better agreement is accomplished. This is certainly the case for the isomers with a fully occupied $N=126$ neutron shell, as would be expected since the calculations are performed for a fully occupied neutron core. But for the core-excited states, the discrepancy is still present. The effective charges of the valence particles can also be empirically determined by forcing agreement between the calculated moments and the measured ones for the single-particle configuration of the nuclei close to ^{208}Pb (Table IV). These empirical quadrupole moments Q_{emp} (Table III) are very close to the calculated effective moments and do not further improve agreement with the experimental values for the core-excited isomers (compare Q_{expt} and Q_{emp}).

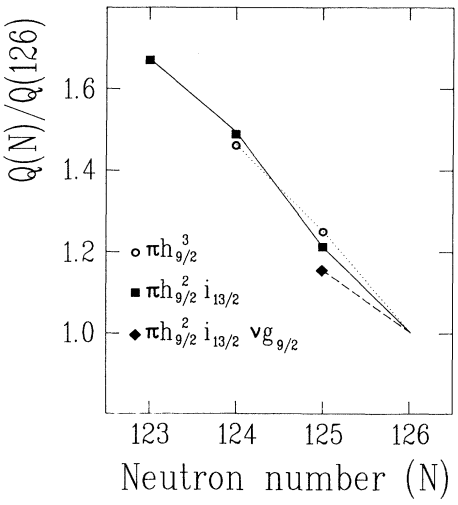

FIG. 5. For each isomeric configuration the quadrupole moment increases for an increasing number of neutron holes in the $N=126$ shell.

TABLE III. Theoretical predictions compared to experimental values for the Q moments of the astatine isomers.

Isomer	Configuration	Q_p (e fm^2)	Q_{eff} (e fm^2)[a]	Q_{emp} (e fm^2)[a]	Q_{expt} (e fm^2)	β_{expt}[b]	β_{core}[c]
^{211}At $\frac{29}{2}^+$ 70 ns	$\pi h_{9/2}^2 \pi i_{13/2}$	−69	−110	−121	101(19)	−0.011(4)	−0.02
^{211}At $\frac{39}{2}^-$ 4.2 μs[d]	$\pi h_{9/2}^2 \pi i_{13/2} \nu p_{1/2}^{-1} \nu g_{9/2}$	−69	−135	−146	191(25)	−0.041(7)	−0.05
^{210}At 11^+ 27 ns	$\pi h_{9/2}^3 \nu p_{1/2}^{-1}$	−31	−47	−51	65(8)	−0.013(5)	−0.02
^{210}At 15^- 580 ns	$\pi h_{9/2}^2 \pi i_{13/2} \nu p_{1/2}^{-1}$	−69	−110	−121	122(12)	−0.019(5)	−0.03
^{210}At 19^+ 4 μs[d]	$\pi h_{9/2}^2 \pi i_{13/2} \nu p_{1/2}^{-2} \nu g_{9/2}$	−69	−135	−146	220(25)	−0.051(6)	−0.05
^{209}At $\frac{21}{2}^-$ 24 ns	$\pi h_{9/2}^3 \nu p_{1/2}^{-2}$	−31	−47	−51	78(8)	−0.018(4)	
^{209}At $\frac{29}{2}^+$ 870 ns	$\pi h_{9/2}^2 \pi i_{13/2} \nu p_{1/2}^{-2}$	−69	−110	−121	150(9)	−0.029(5)	
^{208}At 16^- 1.5 μs	$\pi h_{9/2}^2 \pi i_{13/2} \nu p_{1/2}^{-2} \nu f_{5/2}^{-1}$	−66	−107	−117	169(25)	−0.036(7)	

[a]The effective and empirical quadrupole moments of the valence states used to calculate Q_{eff} and Q_{emp}, are included in Table IV.
[b]The experimental core deformation is calculated with the equations[19] $Q_c^i=(3/\sqrt{5}\pi)ZR^2\{[1+\pi^2(a/R)]^2\beta+(2\sqrt{5}/7\sqrt{\pi})\beta^2\}$, $Q_{\text{def}}^i=Q_c^i+Q_{\text{sp}}^i=Q_{\text{expt}}$, and the sign of Q_{expt} is taken to be negative.
[c]Core deformation proposed by the DIPM (Ref. 9).
[d]The core excited isomers.

Variable effective charges, increasing with the number of neutron holes in the $N=126$ shell, can accomplish agreement with the Q_{expt}; but then, of course, this formalism looses its usefulness. The same behavior is observed throughout the whole region around ^{208}Pb,[3,4] and it is attributed to the increasing core softness as neutrons are removed from the closed shell. The Nilsson scheme for neutrons and protons in the ^{208}Pb region can explain the observed behavior qualitatively. Valence protons and neutrons in orbitals with large spin projection on the symmetry axis correspond to the particles that build up a high-spin isomer. These orbitals clearly gain binding energy by polarizing the core toward oblate deformation. The neutron Nilsson scheme illustrates that much of the $N=126$ core stiffness is attributed to the $\nu p_{1/2}$ orbital; if this orbital is emptied, the core is much easier to polarize.

The core deformations predicted by the DIPM for the isomers in ^{210,211}At are listed in Table III (β_{core}); they are rather small, but because of the high charge and large radii of these nuclei, the effect on the Q moment is large. It is also possible to calculate β_{expt} from the experimental Q moments. Therefore, we take into account the contribution of the deformed core explicitly, rather then using effective charges. In the strong-coupling limit, the spectroscopic Q moment is derived from the intrinsic Q^i value as follows:

$$Q=\frac{3K^2-I(I+1)}{(I+1)(2I+3)}Q^i . \tag{1}$$

For the investigated isomers, no rotation is present and the component of the spin on the intrinsic symmetry axis is I. The intrinsic Q^i has an intrinsic single-particle part Q_{sp}^i, that is calculated with the bare charges for proton and neutron; and an intrinsic core contribution Q_c^i which is a function of the deformation parameter β:

$$Q_c^i=\frac{3}{\sqrt{5\pi}}ZR^2\left[[1+\pi^2(a/R)^2]\beta+\frac{2\sqrt{5}}{7\sqrt{\pi}}\beta^2\right] . \tag{2}$$

The surface thickness and radius are taken to be $a=0.54$ fm and $R=1.2A^{1/3}$ fm, respectively. With the use of Q_{expt}, Q_p, and formula's (1) and (2), experimental values for the core deformation β_{expt} can be computed. The deformation parameters β_{core} determined with the DIPM are in good agreement with the experimental deformations; certainly, the qualitative behavior is very similar. Better quantitative agreement cannot be expected with the use of such a simplified model. The core deformation for the lower-spin isomers is very small and does not pro-

TABLE IV. Empirical and effective Q moments of the valence nucleons.

Orbital	Q_{sp} (e fm^2)[a]	Q_{sp}^{ρ} (e fm^2)[b]	Q_{eff} (e fm^2)[c]	Q_{emp} (e fm^2)[d]
$\nu g_{9/2}$	0	−30.36	−25.35	−29
$\pi i_{13/2}$	−33.76	−33.76	−56.82	−62
$\pi h_{9/2}$	−26.62	−26.62	−40.14	−44
$\nu f_{5/2}^{-1}$	0	+20.56	+19.43	+20

[a]The spherical shell Q moments are calculated with $e_\pi=1$, $e_\nu=0$; the mean-square radii are taken from Ref. 19, $Q_{\text{sp}}=-[(2j-1)/(2j+2)](e_n/e)r^2$, and e_n = effective charge of the nucleon.
[b]The density Q moments are calculated with $e_{\pi,\nu}=1$.
[c]The effective charges to calculate Q_{eff} are taken from Ref. 19.
[d]The empirical Q moments are taken from Ref. 12.

vide a sensitive test as to whether the DIPM mechanism is really present. But for the core-excited isomers, the core deformation is strongly enhanced, as predicted by the DIPM. Even the qualitative agreement between the experimental (β_{expt}) and predicted (β_{core}) deformation parameters is excellent for these two isomers.

Our results are support for the DIPM that attributes the driving force for high-spin isomerism in the Pb region to deformation. Another mechanism that equally well explains the large abundance of high-spin isomers in the Pb region is the particle-octupole vibration coupling.[20] The extra binding energy resulting from this coupling is accurately calculated in the empirical shell model with residual interactions and has roughly the same magnitude as the binding energy predicted by the DIPM.[9]

The admixture of the octupole vibration is experimentally well established; it is needed to explain the strongly enhanced $E3$ decay observed for the high-spin isomers. Experimental results, quadrupole moments, and $E3$ transition rates indicate that both mechanism, deformation and particle-vibration coupling, are present in the high-spin isomer. In principle, they do not exclude each other. The problem is, however, that each mechanism separately predicts the right energy suppression for the observed isomers, and if both interaction energies are added, the energy suppression is much overestimated.

In summarizing the discussion, the quadrupole moments of the isomers with a fully occupied neutron core ($N=126$) are in agreement with the effective charges of the valence particles calculated by configuration mixing with giant resonances of the core.[19] If, however, the neutron shell is broken, the quadrupole moments drastically increase. The core-excited isomers provide the most striking evidence for this behavior, and their deformation is well explained by the DIPM predictions.

The authors would like to express their gratitude to Dr. A. P. Byrne for the many fruitful discussions on the theoretical aspects of high-spin isomers in the lead region.

[1]M. J. A. de Voigt, J. Dudek, and Z. Szymansky, Rev. Mod. Phys. **55**, 949 (1983).
[2]I. Hamamoto, Hyperfine Interact **34**, 33 (1987).
[3]H.-E. Mahnke, Ann. Israel Phys. Soc. **7**, 295 (1984).
[4]H.-E. Mahnke, Hyperfine Interact **34**, 47 (1987).
[5]F. Hardeman, G. Scheveneels, G. Neyens, R. Nouwen, G. S'heeren, M. Van Den Bergh, and R. Coussement, Phys. Rev. C **43**, 130 (1991).
[6]J. Blomqvist, P. Kleinheinz, and P. J. Daly, Z. Phys. A **312**, 27 (1983).
[7]I. Bergström, J. Blomqvist, P. Carlé, B. Fant, A. Källberg, L. O. Norlin, K.-G. Rensfelt, and U. Rosengård, Phys. Scr. **31**, 333 (1985).
[8]G. Andersson, S. E. Larsson, G. Leander, P. Möller, S. G. Nilsson, I. Ragnarsson, S. Åberg, R. Bengtsson, J. Dudek, B. Nerlo-Pomorska, K. Pomorski, and Z. Szymanski, Nucl. Phys. **A268**, 205 (1976).
[9]K. Matsuyanagi, T. Døssing, and K. Neergård, Nucl. Phys. **A307**, 253 (1978).
[10]A. P. Byrne and G. D. Dracoulis, Nucl. Phys. **A391**, 1 (1982).
[11]J. Blomqvist, I. Bergström, C. J. Herrlander, C. G. Lindén, and K. Wikström, Phys. Rev. Lett. **38**, 534 (1977).
[12]E. Dafni, M. Hass, E. Naim, M. H. Rafailovich, A. Berger, H. Grawe, and H.-E. Mahnke, Phys. Rev. Lett. **55**, 1269 (1985).
[13]H.-E. Mahnke, W. Semmler, H. Grawe, H. Haas, and R. Sielemann, Phys. Lett. **122B**, 27 (1983).
[14]B. Fant, T. Weckström, T. Lönnroth, C. J. Herrlander, K. Honkanen, and A. Källberg, Nucl. Phys. **A429**, 296 (1984).
[15]I. Berkes, in *Low-Temperature Nuclear Orientation,* edited by N. J. Stone and H. Postma (North-Holland, Amsterdam, 1986), p. 940.
[16]C. M. Lederer and V. S. Shirley, *Table of Isotopes* (Wiley, New York, 1978).
[17]I. Bergström, C. J. Herrlander, Th. Lindblad, V. Rahkonen, K.-G. Rensfelt, and K. Westerberg, Z. Phys. A **273**, 291 (1975).
[18]M. R. Smorak, Nucl. Data Sheets **31**, 283 (1980).
[19]H. Sagawa and A. Arima, Phys. Lett. B **202**, 15 (1988).
[20]G. D. Dracoulis, C. A. Steed, A. P. Byrne, S. J. Poletti, A. E. Stuchbery, and R. A. Bark, Nucl. Phys. **A462**, 576 (1987).